J Mater Sci (2011) 46:1388–1395
DOI 10.1007/s10853-010-4932-3

Synthesis and characterization of niobium doped hexagonal tungsten bronze in the systems, $Cs_xNb_yW_{1-y}O_3$

Kalpana R. Dey · Tapas Debnath · Claus H. Rüscher · Margareta Sundberg · Altaf Hussain

Received: 7 April 2010 / Accepted: 16 September 2010 / Published online: 16 December 2010

Abstract Samples of nominal compositions, $Cs_{0.25}Nb_yW_{1-y}O_3$ and $Cs_{0.3}Nb_yW_{1-y}O_3$ with $0.0 \leq y \leq 0.25$ and $0.0 \leq y \leq 0.3$ were synthesized using appropriate amounts of Cs_2WO_4, WO_3 and WO_2 in evacuated and closed silica glass tubes at 800 °C. The polycrystalline products contain hexagonal shaped crystals of up to 15 μm diameter as long as $y \leq 0.15$. X-ray powder patterns of the samples reveal the formation of hexagonal tungsten bronze (HTB-I) type phase with $y < 0.1$. A mixture of HTB-I and an analogous less reduced hexagonal tungsten bronze (HTB-II) type phase is seen when $y \geq 0.1$. HTB-II content increases with increasing y, revealing close similarity to bronzoid type phases when $y = x$. Results of SEM/EDX analysis also support a partial substitution of tungsten by niobium in the HTB-I type phase. Infrared absorption and optical reflectivity data shows the effect of increasing amount of non-metallic phase for $y > 0.1$ and the effect of counterdoping by Nb^{5+}/W^{5+} substitution in the metallic HTB-I type phase for $y \leq 0.1$, respectively. Reinvestigations in the system $Rb_{0.3}Nb_yW_{1-y}O_3$ $(0.0 \leq y \leq 0.175)$ show similar results with increasing content of HTB-II type phase related with y.

Dedicated to Professor Lars Kihlborg on the occasion of his 80th birthday.

K. R. Dey · T. Debnath (✉) · C. H. Rüscher
Institute of Mineralogy and Centre of Solid State Chemistry and New Materials (ZFM) of Leibniz University Hannover, Callinstr. 3, 30167 Hannover, Germany
e-mail: tapas.debnath@mineralogie.uni-hannover.de

M. Sundberg
Department of Materials and Environmental Chemistry, Arrhenius Laboratory, Stockholm University, SE-10691 Stockholm, Sweden

T. Debnath · A. Hussain
Department of Chemistry, University of Dhaka, 1000 Dhaka, Bangladesh

Present Address:
K. R. Dey
Department of Chemistry and Biochemistry, Jackson State University, Jackson, MS 39212, USA

Introduction

Tungsten bronzes, M_xWO_3, with M generally an electropositive element and $0.0 < x < 1.0$, have been a subject of intensive study since long for their electric, magnetic and optical properties [1–6]. Magnéli [7] first reported the structure of the heavy alkali metal (K, Rb and Cs) hexagonal tungsten bronzes (HTB), which consists of hexagonal and trigonal tunnels formed by corner sharing WO_6 octahedra. The alkali metal atoms occupy the hexagonal tunnel sites and the metal content, x, is in the range $0.19 \leq x \leq 0.33$ [8].

Tungsten bronzes can also be written as $(M_x(W_y^{5+}W_{1-y}^{6+})O_3)$ which indicates the presence of pentavalent tungsten ions in it. There are reports of substitution of the pentavalent tungsten atoms by other pentavalent atoms such as Nb, Ta and even lower valent atoms [9–14]. The fully substituted (i.e., when $x = y$) phase is known as bronzoid [15], an oxidized analogue of HTB type phase. This substitution of tungsten atoms modifies significantly the properties of bronzes. For example, bronzes show metallic conductivity and superconducting properties depending on the amount of M in it [16–19] whereas bronzoids are insulators, ferroelectrics [20, 21].

Though there are many reports on the study of bronzes and bronzoids, very few of them have so far been published

on the study of the crossover between bronzes and bronzoids. This has incited us to study the effect of systematic niobium substitution in various structure types of bronze. Some results have been published on the HTB bronzes in the systems, $M_xNb_yW_{1-y}O_3$ with M = K and Rb [22], and more recently on the sodium tungsten bronzes system of perovskite type structure (PTB), $Na_{0.8}Nb_yW_{1-y}O_3$ [23]. Here, we report for $Cs_xNb_yW_{1-y}O_3$ system a separation into bronze and "bronzoid" type phases (called in the following HTB-I and HTB-II, respectively) controlled by the Nb/W ratio in the starting composition. Few samples of our earlier preparation [22] of the Rb-system were reinvestigated and its result is also given in this article to compare with Cs-system.

Experimental

Samples with nominal compositions, $Cs_{0.25}Nb_yW_{1-y}O_3$ and $Cs_{0.3}Nb_yW_{1-y}O_3$ with $0.0 \leq y \leq 0.25$ and $0.0 \leq y \leq 0.3$, respectively, were synthesized according to the following reaction:

$$x/2\ Cs_2WO_4 + (1 - x - y/2)WO_3 + 1/2(x - y)\ WO_2 + y/2\ Nb_2O_5 \rightarrow Cs_xNb_yW_{1-y}O_3$$

The starting materials were of high quality reagent grade Cs_2WO_4, Nb_2O_5 (BDH Laboratory Supplies), WO_3 (Ventron GmbH), and WO_2 (Alfa Aesar). Appropriate amount of the reactants was mixed thoroughly in an agate mortar and transferred into clean, dried silica tubes. The silica glass tubes were evacuated (10^{-2} Torr) at room temperature for about 2 h, sealed and then heated in a Muffle Furnace at 800 °C for 7 days. Samples of nominal bronzoid composition (i.e., $x = y$) were also prepared in an oxidizing atmosphere (i.e., heated in air) keeping all the other experimental conditions the same. In all the experiments, samples were quenched to room temperature by taking out the reaction tubes from the furnace.

The X-ray powder patterns of the products were taken by a Philips PW1800 diffractometer (CuKα radiation) and the data were characterized by using Rietveld program (Rietan 2000 and TOPAS 3). Space group, $P6_3/mcm$, was used for the refinement of lattice parameters of HTB-I and HTB-II type phases. For the pyrochlore type phase, space group Fd-3m was used in the calculations. The cell parameters of the pure HTB-I phase were also calculated from X-ray powder photographs taken by Guinier-Hägg focusing camera using CuKα_1 radiation and Si as an internal standard. The cell parameters of pure HTB-I phase obtained from diffractometer and Guinier-Hägg data show excellent agreement within standard deviation.

Samples were studied in a JEOL JSM-820 scanning electron microscope (SEM), which was equipped with a LINK AN 10000 EDS microanalysis system and operated at an accelerating voltage of 20 kV. The SEM specimen was prepared by mounting a small amount of the sample on an aluminium stub with a conducting carbon tape. Co was used as an internal standard. The microanalyses gave information about the Cs:W and Cs:Nb:W ratios in at.%. For the Rb-samples information about the Rb:Nb:W ratios in at.% was obtained. The whole spectra were used in the quantification. From the atomic ratios, the values of x and y in the in $M_xNb_yW_{1-y}O_3$ (M = Cs, Rb) were calculated.

All the samples were investigated by infrared absorption spectroscopy in the range 370–4000 cm^{-1} using Bruker IFS66v FTIR spectrometer. For the transmission IR measurement, the grinded samples were mixed with KBr (1 mg sample in 200 mg KBr) and pressed into pellets. The spectra are given in absorption units with Abs = log (I_o/I), where I_o and I are transmitted intensities through the reference pellet (KBr) and sample pellet diluted with KBr, respectively. The optical reflectivity of the samples were measured in the range of 6000–20000 cm^{-1} against MgO powder as a reference using Bruker IFS88 FTIR spectrometer.

Results and discussion

X-ray study

The XRD patterns of the samples, $Cs_xNb_yW_{1-y}O_3$, are given in Fig. 1 ($x = 0.25$ series) and Fig. 2 ($x = 0.3$ series). The XRD patterns and Rietveld refinement analysis of the data show (Table 1) that Nb-substituted HTB-I type phase could be synthesized with niobium content, $y < 0.1$. Samples with nominal compositions $y \geq 0.1$ reveal a mixture of HTB-I and HTB-II type phases. With the increase of gross niobium content, the amount of HTB-II type phase increases in the mixture. In the system, $Cs_{0.3}Nb_yW_{1-y}O_3$ a third phase, pyrochlore type can also be seen along with HTB-I and HTB-II when $y \geq 0.15$. However, this pyrochlore type phase is absent in the system, $Cs_{0.25}Nb_yW_{1-y}O_3$ even in the composition $x = y$. Samples of gross nominal compositions, $Cs_xNb_yW_{1-y}O_3$, with $x = y = 0.25$ and 0.3 of HTB-II type phase were prepared both in air and also in sealed evacuated tubes. The samples prepared in air are polycrystalline white powder, whereas the samples prepared in sealed evacuated tubes are light bluish in colour. This bluish colour may be due to the fact that samples become slightly reduced under vacuum condition. For $Cs_{0.3}Nb_{0.3}W_{0.7}O_3$ the XRD pattern are almost identical in both cases (Fig. 2), whereas for $Cs_{0.25}Nb_{0.25}W_{0.75}O_3$ a more complex distributions in peak intensities for the sample prepared in vacuum sealed sample (Fig. 1) imply a more complex phase

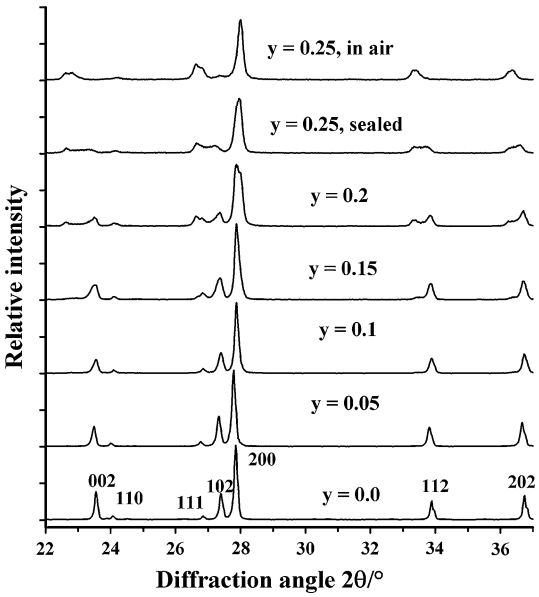

Fig. 1 XRD patterns of the samples of the system, $Cs_{0.25}Nb_yW_{1-y}O_3$

distributions, which could not further be refined. It may be noted that the peaks of the HTB-II type phases for the samples with $y > 0.2$ show significantly larger in halfwidth, which can be related to much smaller crystal sizes compared to those obtained for HTB-I. This may be expected since preparation temperatures of bronzoids are above 1000 °C [13] compared to 800 °C used here.

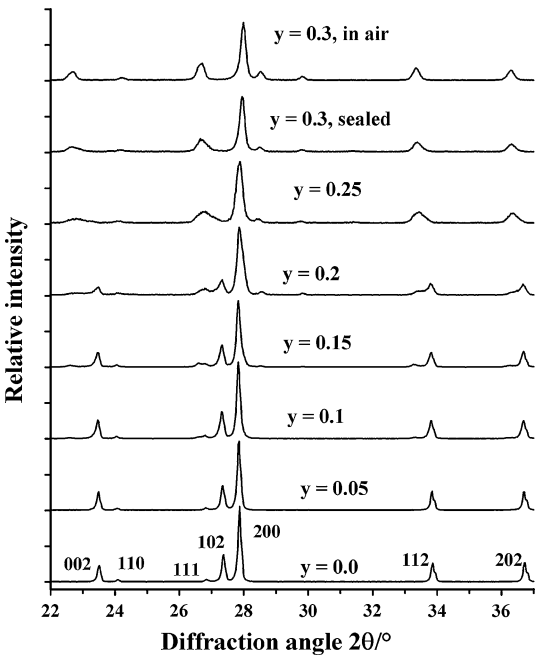

Fig. 2 XRD patterns of the samples of the system, $Cs_{0.30}Nb_yW_{1-y}O_3$

In a previous study [22], using the same preparation conditions as used here, the existence of HTB-II type phase has not been noticed in the related systems $Rb_xNb_yW_{1-y}O_3$, which should be expected according to the new results in the Cs-HTB system. Therefore, we have reinvestigated a few samples of $Rb_{0.3}Nb_yW_{1-y}O_3$ series by XRD. The new results reveal that Rb-HTB system shows a phase separation into HTB-I and HTB-II phases as seen in Cs-HTB system. The Rietveld refinement fit of XRD patterns of four selected samples in Cs-HTB and Rb-HTB systems are shown in Fig. 3. The results of $Rb_{0.3}Nb_{0.15}W_{0.75}O_3$ show the presence of HTB-I and HTB-II type phases, whereas for $Rb_{0.3}Nb_{0.05}W_{0.95}O_3$ only HTB-I is observed similarly to the finding in Cs-HTB system.

The lattice parameters obtained for HTB-I type phase in this investigation are in good agreement with the previously reported data [22]. With a gradual increase in Nb/W ratio, a systematic increase in *c*-lattice parameter and a decrease in *a*-lattice parameter values could be expected assuming a solid solution type effect between the $y = 0$ and $x = y$ end members. However, such trend was not obviously in the lattice parameter with *y*, which could be related to a distribution in the chemical composition of crystals from the same batch and the limited amount of Nb substitution in HTB-I phase. The XRD patterns and Rietveld refinement analysis of the samples with nominal compositions $x = y$ should have HTB-II type as expected; however, the results are different especially for $Cs_{0.25}Nb_{0.25}W_{0.75}O_3$, which shows a mixture of two phases. Such results are also observed even if the sample is prepared in air. The Rietveld analysis of the second phase in the sample gives a different lattice parameters than HTB-II (see footnote indicator "a" marked in the Table 1).

SEM/EDX microanalysis study

Results of SEM/EDX microanalysis of series of samples under consideration were reported in detail by Dey [24]. The SEM micrographs in Fig. 4a and b show that crystals with hexagonal shape were formed in all the examined samples. The EDS analyses of such crystals showed an average Cs content of $x \approx 0.3$. A slightly larger Cs content for nominal $x = 0.3$ samples compared to $x = 0.25$ samples is observed which could also be concluded from the variation in lattice parameters as reported for the $y = 0$ samples [8]. The Nb contents were found to be in the range $0.0 \leq y \leq 0.1$. The SEM results in Table 2 indicate that substitution of niobium for tungsten can take place, thereby forming two phases of hexagonal tungsten bronzes type (HTB-I and HTB-II) with significantly different Nb-content and thus supporting the X-ray results above. The high Nb-content in HTB-II indicates that this phase is formed in the region close to the bronzoid $Cs_{0.3}Nb_{0.3}W_{0.7}O_3$.

Table 1 X-ray results of the systems, $Cs_xNb_yW_{1-y}O_3$ and $Rb_xNb_yW_{1-y}O_3$

Nominal composition	Rietveld refinement results of different phases from XRD data					
	HTB-I			HTB-II		
	Amount (%)	Cell parameters		Amount (%)	Cell parameters	
		a (Å)	*c* (Å)		*a* (Å)	*c* (Å)
$Cs_{0.25}WO_3$	100	7.4216(1)	7.5840(1)	–	–	–
$Cs_{0.25}Nb_{0.05}W_{0.95}O_3$	100	7.4247(1)	7.5885(1)	–	–	–
$Cs_{0.25}Nb_{0.1}W_{0.9}O_3$	96	7.4125(2)	7.5875(2)	4	7.3706(8)	7.7976(9)
$Cs_{0.25}Nb_{0.15}W_{0.85}O_3$	88	7.4031(2)	7.6017(2)	12	7.3693(4)	7.8187(4)
$Cs_{0.25}Nb_{0.2}W_{0.8}O_3$	65	7.4044(2)	7.6085(2)	35	7.3689(2)	7.8460(2)
$Cs_{0.25}Nb_{0.25}W_{0.8}O_3$[a]	–	–	–	46	7.3889(5)	7.6703(5)
				54	7.3686(3)	7.8453(2)
$Cs_{0.3}WO_3$	100	7.4178(1)	7.5982(1)	–	–	–
$Cs_{0.3}Nb_{0.05}W_{0.95}O_3$	100	7.4175(1)	7.5982(1)	–	–	–
$Cs_{0.3}Nb_{0.1}W_{0.9}O_3$	95	7.4113(7)	7.5979(5)	5	7.3799(4)	7.8699(5)
$Cs_{0.3}Nb_{0.15}W_{0.85}O_3$[b]	86	7.4144(5)	7.5987(4)	14	7.3770(2)	7.8707(2)
$Cs_{0.3}Nb_{0.2}W_{0.8}O_3$[b]	65	7.4156(2)	7.6152(2)	35	7.3822(2)	7.8128(2)
$Cs_{0.3}Nb_{0.25}W_{0.75}O_3$[a,b]	–	–	–	25	7.39643(3)	7.6983(3)
				75	7.3848(3)	7.8124(2)
$Cs_{0.3}Nb_{0.3}W_{0.7}O_3$	–	–	–	92	7.3846(3)	7.8383(2)
				8[b]	10.3920(7)	–
$Rb_{0.3}WO_3$	100	7.3919(1)	7.5586(1)	–	–	–
$Rb_{0.3}Nb_{0.05}W_{0.95}O_3$	100	7.3913(1)	7.5552(1)	–	–	–
$Rb_{0.3}Nb_{0.07}W_{0.93}O_3$	100	7.3917(1)	7.5545(1)	–	–	–
$Rb_{0.3}Nb_{0.125}W_{0.875}O_3$	93	7.3913(1)	7.5464(1)	7	7.3398(9)	7.8000(2)
$Rb_{0.3}Nb_{0.15}W_{0.85}O_3$	83	7.3914(1)	7.5499(2)	17	7.3375(6)	7.8000(9)
$Rb_{0.3}Nb_{0.175}W_{0.825}O_3$	81	7.3905(1)	7.5496(2)	19	7.3346(1)	7.8000(8)

[a] Such composition in principle should give one HTB-II type phase only

[b] Trace amount of Pyrochlore type phase seen in the XRD

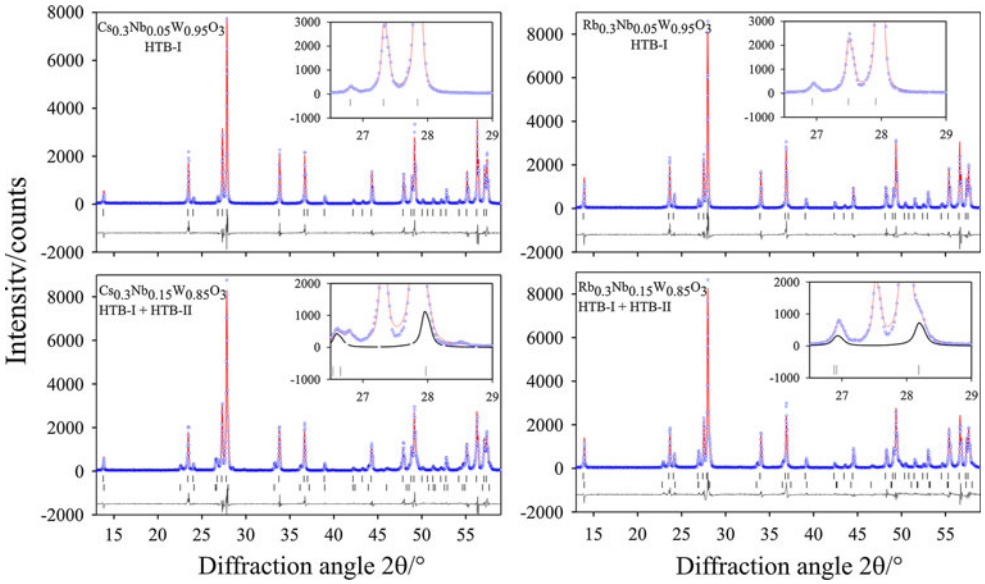

Fig. 3 Observed (*dotted*) and refined (*solid line*) XRD patterns of the samples, $M_{0.30}Nb_yW_{1-y}O_3$ (M = Cs, Rb, $y = 0.05, 0.15$). The corresponding difference curves and peak positions (*bars*) are also shown in each case. *Inset* shows an enlarge view where the *solid line* represents the contribution of HTB-II type phase

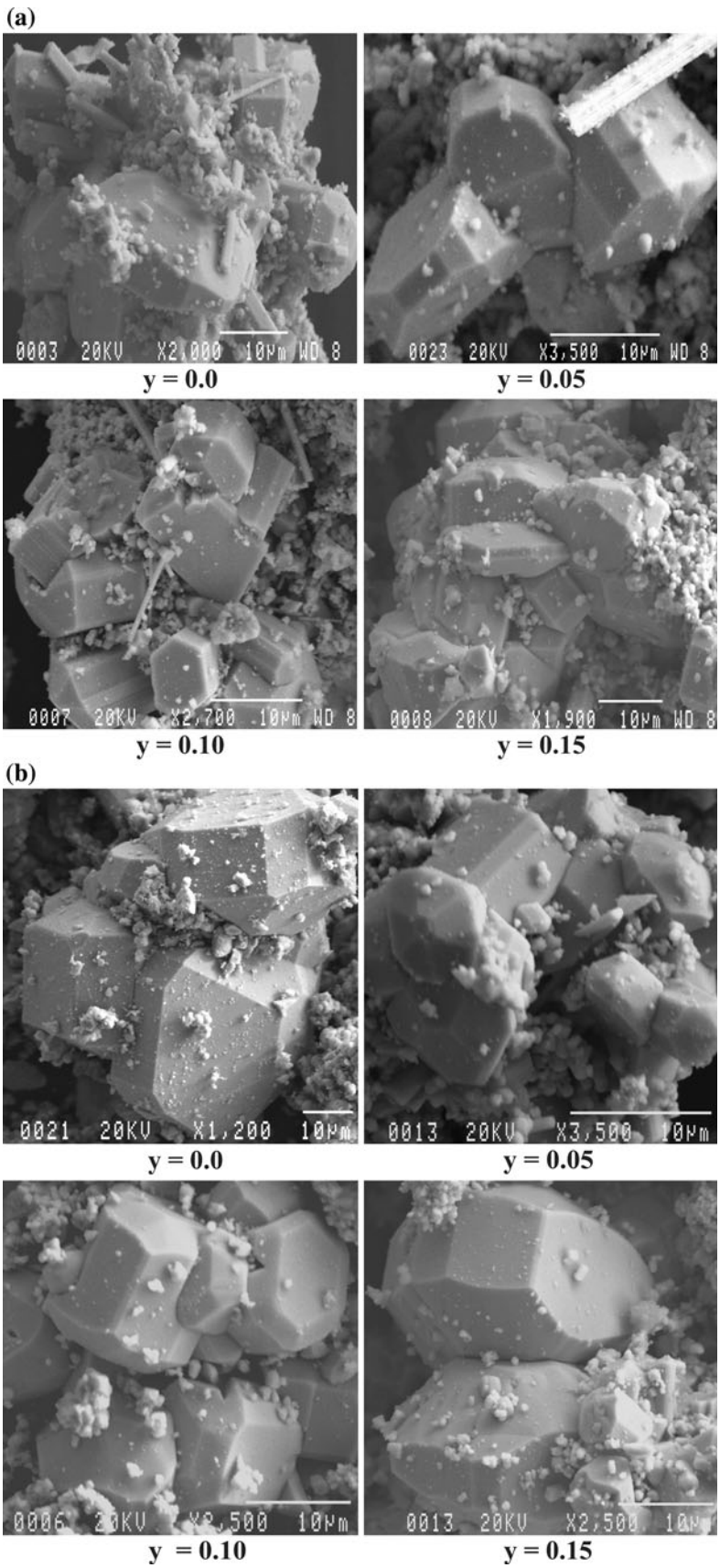

Fig. 4 Scanning electron micrographs (SEM) of some selected samples of **a** $Cs_{0.25}Nb_yW_{1-y}O_3$ and **b** $Cs_{0.30}Nb_yW_{1-y}O_3$ systems (pictures taken from [24]

Table 2 SEM/EDX results of $Cs_xNb_yW_{1-y}O_3$ and $Rb_xNb_yW_{1-y}O_3$ (data collected from [24])

Starting composition	SEM/EDX	
	x_{min}–x_{max} x_{mean}	y_{min}–y_{max} y_{mean}
$Cs_{0.25}WO_3$	0.24–0.29 $x_{mean} = 0.27$	–
$Cs_{0.25}Nb_{0.05}W_{0.95}O_3$	0.24–0.33 $x_{mean} = 0.28$	0.03–0.13 $y_{mean} = 0.06$
$Cs_{0.25}Nb_{0.10}W_{0.90}O_3$	0.23–0.33 $x_{mean} = 0.28$	0.03–0.14 $y_{mean} = 0.09$
$Cs_{0.25}Nb_{0.15}W_{0.85}O_3$	0.25–0.32 $x_{mean} = 0.29$	0.09–0.16 $y_{mean} = 0.13$
$Cs_{0.25}Nb_{0.20}W_{0.80}O_3$	–	–
$Cs_{0.30}WO_3$	0.28–0.33 $x_{mean} = 0.31$	–
$Cs_{0.30}Nb_{0.05}W_{0.95}O_3$	0.28–0.33 $x_{mean} = 0.31$	0.02–0.11 $y_{mean} = 0.07$
$Cs_{0.30}Nb_{0.10}W_{0.90}O_3$	0.30–0.33 $x_{mean} = 0.32$	0.02–0.14 $y_{mean} = 0.10$
$Cs_{0.30}Nb_{0.15}W_{0.85}O_3$	0.27–0.33 $x_{mean} = 0.30$	0.08–0.15 $y_{mean} = 0.12$
$Rb_{0.30}Nb_{0.125}W_{0.875}O_3$	0.29–0.37 $x_{mean} = 0.33$	0.07–0.11 $y_{mean} = 0.09$
$Rb_{0.30}Nb_{0.15}W_{0.85}O_3$	0.32–0.38 $x_{mean} = 0.35$	0.06–0.11 $y_{mean} = 0.09$
$Rb_{0.30}Nb_{0.175}W_{0.825}O_3$	0.31–0.39 $x_{mean} = 0.35$	0.08–0.14 $y_{mean} = 0.11$

However, it is clear from the electron microscopy study that niobium has been incorporated in HTB-I type phase. The EDS-study also showed that the Cs:(Nb/W) content varied from crystal to crystal within a sample. The x_{mean} and y_{mean} values given in Table 2 are based on 10–20 analyzed crystals from each sample. Though there was a scattering in the measured values of x and y from crystal to crystal of the same batch, however, the accuracy in each measurement point was better than $\pm/-0.025$. It is expected that a much better value of standard deviation will be observed when the study of the samples will be completed by the combination of electron diffraction and microanalysis in TEM. The results of this study will be published elsewhere.

SEM studies of the $Rb_{0.3}Nb_yW_{1-y}O_3$ with $0.125 \leq y \leq 0.175$ showed a Rb-content of approximately 0.1 thus confirming the replacement of niobium for tungsten in the HTB-I phase. In particular, the effect of niobium substitution seems not to increase about 0.1 showing that the phase limit of HTB-I type phase has been reached under the present synthesis conditions. This supports earlier results of Rietveld refinements for samples of $Cs_xNb_yW_{1-y}O_3$ with $x = 0.3$, 0.25 and $y = 0.1$ [25] and also for $Rb_{0.3}Nb_yW_{1-y}O_3$ with $y = 0.1$ and 0.2 [26]. However, for

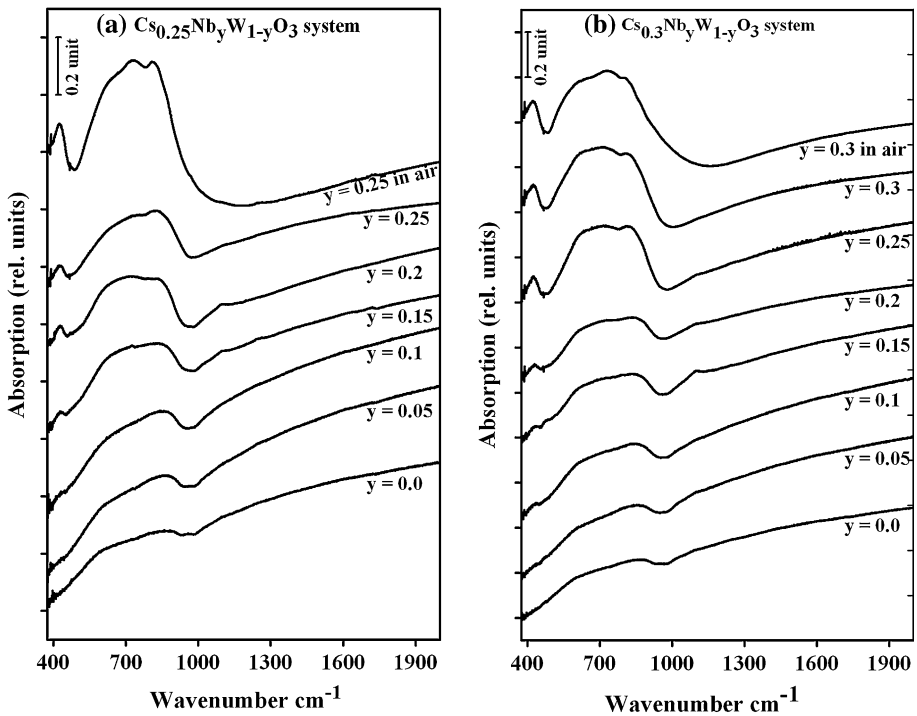

Fig. 5 The IR absorption spectra (KBr method) of **a** $Cs_{0.25}Nb_yW_{1-y}O_3$ and **b** $Cs_{0.30}Nb_yW_{1-y}O_3$ systems. The spectra are shifted *vertically* for better comparison

sample of nominal composition $Rb_{0.3}Nb_{0.2}W_{0.8}O_3$ the niobium content could have been overestimated in the Rietveld refinement.

Optical spectroscopy study

The IR absorption spectra of the system, $Cs_xNb_yW_{1-y}O_3$, are given in the Fig. 5. The spectrum of niobium free HTB-I phase has a weak broad phonon absorption band below 1000 cm^{-1}, which is related to surface effects of the sample. The intensity of phonon absorption increases with the increase of $y > 0.1$, which is due to the increasing amount of HTB-II type phase. The spectra observed for the samples $Cs_{0.25}Nb_{0.25}W_{0.75}O_3$ and $Cs_{0.3}Nb_{0.3}W_{0.7}O_3$ are in good agreement with powder related spectra published by Maczka et al. [27].

The optical reflectivity of the series of powder samples, $Cs_xNb_yW_{1-y}O_3$, with $x = 0.3$ and 0.25 was measured in the spectral range between 6000 and 20000 cm^{-1} (Fig. 6a, b). The pure HTB-I (i.e., $y = 0.0$) sample shows two pronounced minimum at about 16000 and 10000 cm^{-1} together with a sharp increase in reflectivity towards lower wavenumber. It is seen that for the $Cs_{0.25}WO_3$ sample these minima are shifted towards lower values by about 500 cm^{-1} compared to those of $Cs_{0.3}WO_3$ sample. The observed shape of the spectra agrees well using the modelling of single crystal data [28] by the Drude free carrier model describing the plasma edge of doped electrons. The minimum in reflectivity is related to the number of doped electrons for the reflectivity component with E//c, R_c. The structure in the reflectivity on the low wavenumber side of the minimum is related to the E⊥c component, R_a. This is shown in Fig. 6a (dashed lines) using single crystal parameter values for $Cs_{0.3}WO_3$ and $Cs_{0.2}WO_3$ from [28] calculating the reflectivity curve as $\langle R \rangle = 1/3\ R_c + 2/3\ R_a$. For Cs_xWO_3 with $x = 0.2$ and 0.3 there is a relative shift in the plasma edges of about 1000 cm^{-1}. The increase in electron concentration can be related formally to the number of W^{5+} states as $Cs_xW_x^{5+}W_{1-x}^{6+}O_3$. Consequently, the effect of counter doping is given by the substitution of Nb^{5+} against W^{5+} as $Cs_xNb_y^{5+}W_{x-y}^{5+}W_{1-x}^{6+}O_3$. Thus, with a substitution of $y = 0.1$, a shift towards lower wavenunmber of about 1000 cm^{-1} equivalent to $x = 0.3$ to $x = 0.2$ can be expected as is seen in the spectra. For $y > 0.1$ no further shift is observed indicating the limit of counter doping in these cases. The change in spectral features for $y > 0.1$ is related to the decreasing and increasing contribution of HTB-I and HTB-II, respectively. The spectral features are similar also in the HTB system, $Rb_xNb_yW_{1-y}O_3$ [22], which has been related to the effect of counter doping, too. It has been reported by Hussain et al. [22] that the saturation in shift at about $x = 0.1$ could be due to the effect of localisation effect of free carriers. Now, it can be concluded that such a metal to insulator transition does not occur in HTB-I under the present synthesis conditions. Instead, HTB-II is formed while reaching the phase stability limit of HTB-I at y about 0.1 in these systems. Moreover, it may be noted that the main spectral feature in the metallic tungsten bronzes cannot be fitted uniquely with the Drude-free carrier model. Instead, an oscillator function

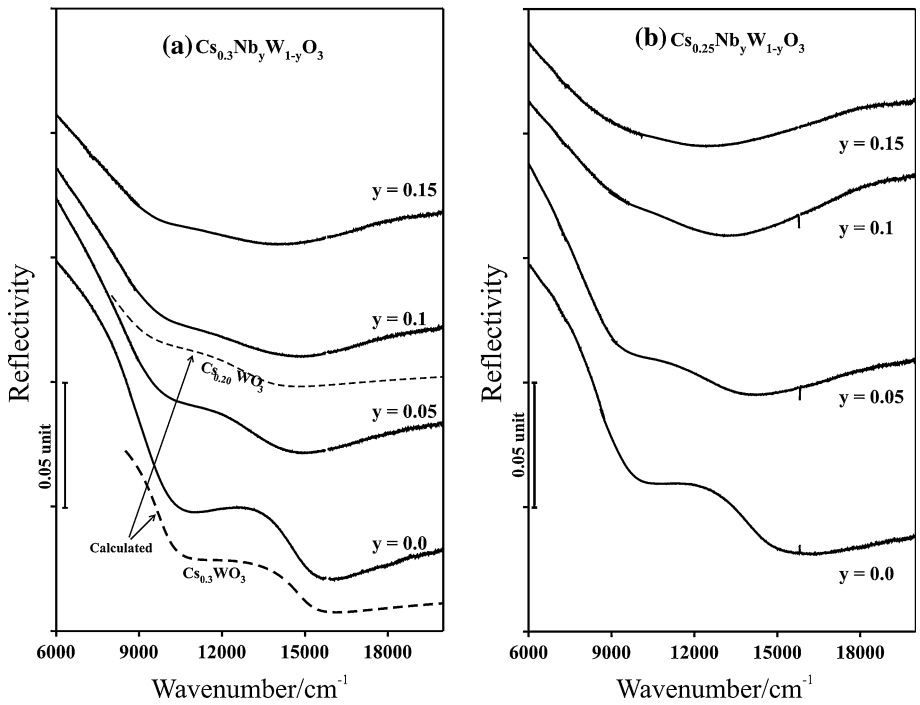

Fig. 6 Reflectivity spectra of samples of **a** $Cs_{0.30}Nb_yW_{1-y}O_3$ and **b** $Cs_{0.25}Nb_yW_{1-y}O_3$ systems. The spectra are shifted *vertically* for better comparison. The *dashed curves* in (**a**) are the calculated reflectivity using single crystal data [28]

with a low lying transversal optical mode becomes more appropriate assuming the formation of intermediate sized polarons [29, 30]. Irrespective of these details, the relative shift in the plasma edge is still to be used as sensitive analytical tool as seen here.

Conclusion

The XRD data of samples prepared in the compositional systems $Cs_{0.25}Nb_yW_{1-y}O_3$ and $Cs_{0.3}Nb_yW_{1-y}O_3$ with $0.0 \leq y \leq 0.25$ and $0.0 \leq y \leq 0.3$, $Rb_{0.3}Nb_yW_{1-y}O_3$ with $0.0 \leq y \leq 0.175$ show that for $y > 0.1$, a second hexagonal tungsten bronze type phase appears which could be identified as bronzoid HTB-II type phase. Lattice parameter refinement of XRD data of the system $Cs_xNb_yW_{1-y}O_3$ show no significant change in values for single HTB-I with y. The effect of limited substitution could be characterized using SEM/EDX analytical work. Moreover, the limited shift in the plasma edge effect towards lower wavenumbers shows the effect of counter doping by Nb^{5+}/W^{5+} substitution.

Acknowledgements This study is supported by DFG (RU 764/4-1) and KRD is thankful to DFG for financial support of her renewed stay at Leibniz University Hannover (LUH). AH thanks Alexander von Humboldt Stiftung for financial support through a collaborative research program (V-FOKOOP/DEU/1062067/Hussain). TD and KRD are grateful to "Land Niedersachsen, Germany" for funding Ph.D. research work within "Lichtenberg Stipendium".

References

1. Dickens PG, Whittingham MS (1968) Quart Rev Chem Soc 22:30
2. Hussain A (1978) Chem Commun Univ Stockholm 2:1
3. Labbe Ph (1992) Key Eng Mater 68:293
4. Granqvist CG (2000) Sol Energy Mater Sol Cells 60:201
5. Mann M, Shter GE, Reisner GM, Grader GS (2007) J Mater Sci 42:1010. doi:10.1007/s10853-006-1384-x
6. Wang Q, Cao F, Chen Q (2006) J Mater Sci 41:285. doi:10.1007/s10853-005-2956-x
7. Magnéli A (1953) Acta Chem Scand 7:315
8. Hussain A (1978) Acta Chem Scand A32:479
9. Debnath T, Roy SC, Rüscher CH, Hussain A (2009) J Mater Sci 44:179. doi:10.1007/s10853-008-3101-4
10. Yanovskii VK, Voronkova VI, D'yakov VA (1976) Sov Phys Crystallogr 21:559
11. Sabatier R, Baud G (1972) J Inorg Nucl Chem 34:873
12. Minaeva GN, Voronkova VI, Yanovskii VK (1979) Sov Phys Crystallogr 24:276
13. Sharma R (1985) Mat Res Bull 20:1373
14. Klimova IP, Voronkova VI, Yanovski VK (1995) Inorg Mat 31:245
15. Magnéli A (1989) In: 12th European Crystallographic Meeting, Moscow
16. Cadwell LH, Morris RC, Moulton WG (1981) Phys Rev B 23:2219
17. Brusetti R, Bordet P, Marcus J (2003) J Solid State Chem 172:148
18. Skokan MR, Moulton WG, Morris RC (1979) Phys Rev B 20:3670
19. Stanley RK, Morris RC, Moulton WG (1979) Phys Rev B 20:1903
20. Maczka M, Hanuza J, Waskowska A (2003) J Raman Spectrosc 34:432
21. Stefanovich SYu, Bazarova ZhG, Batueva IS, Mokhosoev MV (1990) Sov Phys Crystallogr 35:692
22. Hussain A, Ul-Monir A, Murshed MM, Rüscher CH (2002) Z Anorg Allg Chem 628:416
23. Debnath T, Rüscher CH, Gesing ThM, Koepke J, Hussain A (2008) J Solid State Chem 181:783
24. Dey KR (2004) In: Ph.D. Thesis, Leibniz University of Hannover, Germany
25. Dey KR, Gesing ThM, Rüscher CH, Hussain A (2002) Z Kristallogr NCS 217:461
26. Gesing ThM, Rüscher CH, Hussain A (2001) Z Kristallogr NCS 216:37
27. Maczka M, Hanuza J, Majchrowski A (2001) J Raman Spectrosc 32:929
28. Hussain A, Gruehn R, Rüscher CH (1997) J Alloys Compd 246:51
29. Debnath T (2008) In: Ph.D. Thesis, Leibniz University of Hannover, Germany
30. Debnath T, Rüscher CH, Robben L (2009) Z Kristallogr Suppl 29:131